Properties of deep convection in tropical continental, monsoon, and oceanic rainfall regimes

Weixin Xu[1] and Edward J. Zipser[2]

Received 5 February 2012; revised 8 March 2012; accepted 9 March 2012; published 7 April 2012.

[1] This study compares vertical structures and properties of deep convection for continental, monsoonal, and oceanic rainfall regimes based on 13-yr TRMM measurements. There is evident regime separation in convective structures and properties of deep convection: continental and oceanic regimes are at two ends of the spectrum, with monsoon regimes intermediate between them. For example, most of the continental rainfall (70–80%) is contributed by storms having 40-dBZ radar echoes reaching above 6-km, strong ice scattering signature, and lightning flashes. This indicates that continental convection is dominated by robust mixed-phase processes such as freezing of raindrops or riming of graupel supported by strong updrafts. In contrast, less monsoon rainfall (~40%) or very limited oceanic rainfall (~10%) involves these vigorous microphysical processes in mixed-phase regions. Though monsoons are intermediate in convective intensity, both current and previous studies show that their active periods are closer to oceanic regimes and their break periods are slightly closer to continental regimes. In short, this study offers novel guidance for categorization of convective properties of three regime archetypes and will be important for future regional, climatological, and modeling studies. **Citation:** Xu, W., and E. J. Zipser (2012), Properties of deep convection in tropical continental, monsoon, and oceanic rainfall regimes, *Geophys. Res. Lett.*, *39*, L07802, doi:10.1029/2012GL051242.

1. Introduction

[2] Convection, especially deep convection (or "hot towers"), plays a very important role in transporting the net energy gain at the surface of equatorial regions to the upper atmosphere and thence to higher latitudes [*Riehl and Simpson*, 1979; *Tao et al.*, 1990]. Accurate descriptions of convection, precipitation and microphysics are essential for the calculation of the vertical profile of latent heating [*Mapes and Houze*, 1995], cumulus parameterizations or super-parameterization [*Arakawa*, 2004], and satellite rainfall retrievals [*Petersen and Rutledge*, 2001]. Statistics of the convective structures and their rainfall contribution may offer a roadmap for model simulations either on mesoscale or climate scale [*Lang et al.*, 2007; *Varble et al.*, 2011].

[3] The convection type of tropical rainfall is often divided into two archetypical regimes: continental and maritime [*Zipser and Lutz*, 1994; *Mohr and Zipser*, 1996; *Rosenfeld and Lensky*, 1998; *Petersen and Rutledge*, 2001; *Williams and Stanfill*, 2002]. The continental regime typically features intense convection, frequent lightning, and strong updrafts, with a large fraction of precipitation involving ice-processes. The maritime rainfall typically features weak-to-moderate convection with a large fraction of precipitation contributed by low-level "warm-rain" processes through collision and coalescence. Convective processes leading to tropical monsoon rainfall have been shown to combine both of these two convective regimes [*Williams et al.*, 2002; *Petersen et al.*, 2002; *Cifelli et al.*, 2002; *Xu et al.*, 2009; *Lang et al.*, 2010]. Active monsoon convection is more maritime-like, while the break periods are often closer to continental convection. In addition, seasonal (or intraseasonal) and regional-scale variations in atmospheric forcing could result in different occurrence, intensity, and convective structures of convection [*Petersen and Rutledge*, 2001; *Petersen et al.*, 2002; *Cifelli et al.*, 2002; *Xu et al.*, 2009; *Lang et al.*, 2010].

[4] Convective properties and structures of precipitation systems have been investigated extensively case by case, period by period, or on regional to global scale. However, convection type and structures of continental, monsoonal, and oceanic rainfall over the globe have never been placed in the same context using statistics over long periods. This paper is motivated to examine variations of convection types of those three archetypical rainfall regimes over the tropics using 13 years of TRMM observations. In addition, 12 years of monsoon convection in actives and breaks over South China and North Australia are placed under the global regime context.

2. Data and Methodology

2.1. TRMM Precipitation Features (PFs) and Convection Proxies

[5] A 13-yr (1998 through 2010) precipitation feature database [*Liu et al.*, 2008] based on the TRMM version-6 satellite data is used in this study. In particular, radar defined PFs are examined. Extremely small (<200 km^2) features are excluded in this study, since they are comprised of only a few pixels and contribute only a few percent of total rainfall [*Liu et al.*, 2008]. Several PF parameters are selected for proxies of convective properties. The maximum height of 20-dBZ radar reflectivity is an indicator of how high the updraft can loft precipitation-size ice particles. On the other hand, maximum height of 40-dBZ radar echo is a better indicator of convective intensity or updraft speed. The vertical profile of the maximum radar reflectivity (VPRR) in a PF is a direct indicator of the vertical structure of the convective core of precipitation systems [*Zipser and Lutz*, 1994]. In addition, lightning flash counts are defined as all the lightning flashes occurring in a PF,

[1]Earth System Science Interdisciplinary Center, University of Maryland, College Park, Maryland, USA.
[2]Department of Atmospheric Sciences, University of Utah, Salt Lake City, Utah, USA.

Copyright 2012 by the American Geophysical Union.
0094-8276/12/2012GL051242

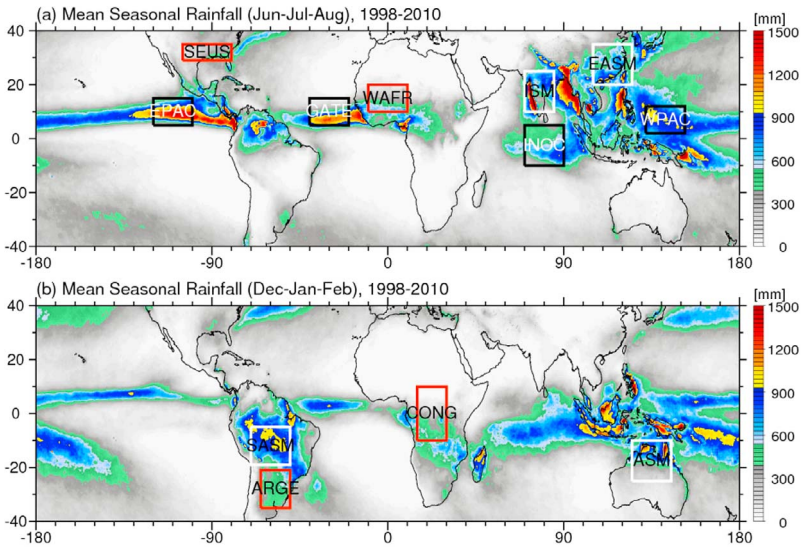

Figure 1. Mean seasonal rainfall (based on TRMM 3B42 rainfall product) during 1998–2010 in (a) north hemisphere summer (JJA) and (b) south hemisphere summer (DFM). Overlaid white, red, and blue boxes represent study regions for monsoon, continental, and oceanic regimes, respectively.

indicating total lightning activity within the feature. Last but not least, polarization corrected temperature (PCT) at 37-GHz from TMI measurements is used as a scattering signature from large ice particles, e.g., hail or large graupel [*Cecil*, 2011; *Cecil and Blankenship*, 2012].

2.2. Defining Tropical Rainfall Regimes

[6] Three rainfall regimes in the broad tropics (35 S to 35 N) are defined and selected for analysis. The monsoon regime includes the East Asian Summer Monsoon (EASM) [*Chang*, 2004], Indian Summer Monsoon (ISM) [*Suppiah*, 1992], Australia Summer Monsoon (ASM) [*Gadgil*, 2003], and South American Summer Monsoon (SASM) [*Zhou and Lau*, 1998]. EASM and ISM are active from June to August (JJA), while ASM and SASM are mature in December-January-February (DJF). EASM, ISM, ASM, and SASM are defined in their mature periods in regions of (20–35 N; 105–125 E), (15–25 N; 75–90 E), (10–25 S; 125–145 E), and (5–20 S, 55–75 W), respectively. It is well known that intense convection, overshooting storms, and high flash rate thunderstorms frequently occur over certain continental regions [*Zipser*, 1994; *Zipser et al.*, 2006]. Detected PFs over four regions in their peak warm seasons is selected as continental regimes: Congo (CONG; 10 S–10 N, 15–30 E) in March-April-May; West Africa (WAFR; 10–20 N, 10 W–10 E) in JJA; Argentina (ARGE; 20–35 S, 50–65 W) in DJF; Southeast US (SEUS; 30–35 N, 80–105 W) in JJA. Finally, convection over four tropical oceanic regions during JJA is chosen as oceanic regimes. Specific regions are: Western Pacific warm pool (WPAC; 2–12 N, 132–152 E), Indian Ocean (INOC; 10 S–5 N, 70–90 E), GATE ocean (GATE; 5–15 N, 20–40 W), and East Pacific (EPAC; 5–15 N, 100–120 W). All these regions are marked in Figure 1, while PF samples are shown in Table 1.

2.3. Defining Active and Break Monsoon Periods

[7] Active and break periods of EASM and ASM during 1998–2009 are examined. Active monsoon periods over EASM (South China; 20–28 N, 105–125 E) are defined as periods with significant monsoon rainbands [*Xu et al.*, 2009], while breaks are defined as periods without any such rainbands. Active periods of ASM are defined as periods experiencing westerly flows (>3 m s^{-1}) at 700-hPa using NCEP reanalysis data. On the other hand, break periods are defined as periods with 700-hPa easterlies (<−3 m s^{-1}). PF populations during each active/break period are listed in Table 1.

3. Results

3.1. Rainfall Contribution by Storm Types

[8] Generally, rainfall amounts of selected regions are in the ascending sequence of continental, monsoonal, and oceanic regimes (Figure 1). Figure 2 shows the cumulative frequency of rainfall contribution by precipitation systems categorized by storm size, precipitation top, top of intense echo, and total lightning flashes. Generally, continental,

Table 1. Population of Precipitation Features in Regions of Specific Regimes or Periods

Regimes/Periods	PFs Number
Monsoon	
EASM	28,963
ISM	20,622
ASM	22,788
AMAZ	49,331
Continent	
SEUS	21,108
WAFR	10,480
CONG	17,198
ARGE	23,359
Ocean	
WPAC	43,702
INOC	41,521
GATE	28,021
EPAC	39,936
Active/Break	
EASM-active	4375
EASM-break	7469
ASM-active	4072
ASM-break	6920

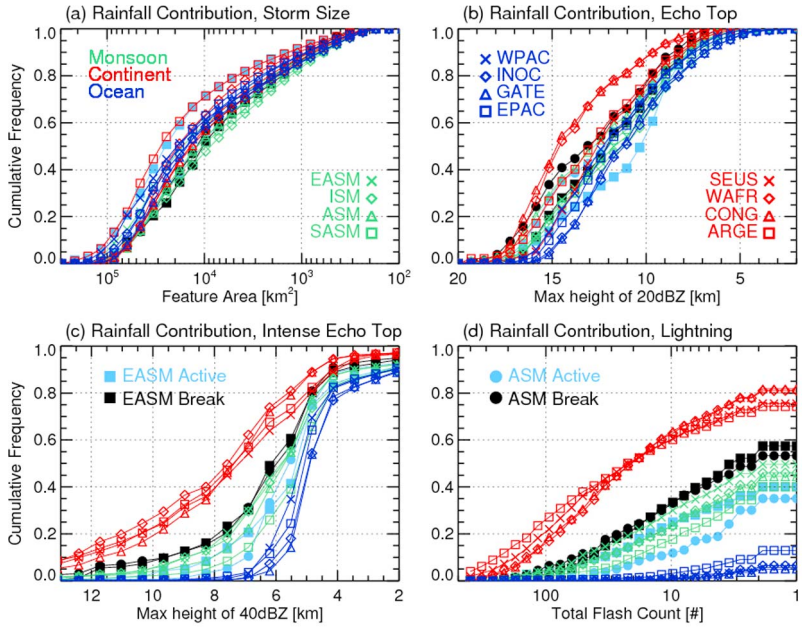

Figure 2. Cumulative distribution frequency (CDF) of rainfall (volumetric rain defined by TRMM 2a25) fraction contributed by precipitation systems categorized by (a) storm size, (b) echo top, (c) intense echo top, and (d) lightning in specific continental (red curves), monsoon (green curves), oceanic (blue curves) regimes, and a set of active/break periods (curves with filled squares or circles).

monsoon, and oceanic rainfall regimes have similar rainfall fractions contributed by horizontal (size) or vertical (echo top) storm extent (Figures 2a and 2b), but have different fractions of rainfall contributed by PFs with intense convection or lightning (Figures 2c and 2d). Most of the rainfall (80%) on Earth falls from PFs exceeding the size criteria of mesoscale convective systems (e.g., 2000 km^2). More than half of the rainfall comes from systems with deep convection, i.e., max height of 20 dBZ echoes reaching above 12 km. These two convective characteristics are regime invariant. The differences between continental, monsoon, and oceanic convection seem to lie not in size or vertical extent of radar echoes, but in the proxies for convective intensity.

[9] Figure 2c shows evident regime variations on rainfall contribution by convection intensity and mixed-phase microphysical processes. Rainfall contribution by storms involving strong mixed-phase processes (i.e., freezing of raindrops and riming) differs greatly among different regimes. For example, using rainfall fraction from 40 dBZ echoes exceeding 6 km in altitude as a metric, 70, 40, and 10% of continental, monsoon, and oceanic rainfall, respectively, comes from PFs with such intense convection. Therefore, monsoon rainfall is intermediate between continental and oceanic rainfall properties, though the SASM convection is closer to oceanic convection (Figure 2c).

[10] Dramatic regime differences are also shown from the perspective of rainfall contribution by lightning activity (Figure 2d). Rainfall contribution from storms with lightning is 80%, 40%, and 10% for continental, monsoon, and oceanic regimes, respectively. These numbers are quite close to those of rainfall contribution by storms with intense echo top above freezing level. In fact, lightning activity also strongly indicates robust mixed-phase microphysical processes [*Zipser*, 1994]. The rainfall-lightning relationships could be very different among different regimes, thus their application in rainfall retrievals.

3.2. Convective Vertical Structures and Microphysics

[11] Figure 3 shows the convective vertical structures (shown by radar vertical profiles). Convective vertical structures of different rainfall regimes fall into three distinct groups, particularly for more extreme precipitation systems (top 10–20%; Figures 3a and 3b). Continental convection presents the strongest profiles of radar echoes, especially above the freezing level indicating strong updraft and existence of large ice particles [*Zipser and Lutz*, 1994; *Zipser et al.*, 2006]. Note that "strongest" VPRR corresponds to higher values of reflectivity throughout the plot. On the other end, oceanic storms have the weakest vertical profiles with dBZ decreasing more rapidly than continental and monsoon systems with height above the freezing level. This is often attributed to updrafts too weak to loft large ice particles or precipitation-size supercooled liquid droplets above the freezing level. Vertical profiles of monsoon convection are intermediate between those of continents and oceans.

[12] Specifically, when all continental, monsoon, and oceanic regimes are considered, their top 10% storms have about 43, 36, and 28 dBZ radar reflectivities at the level of −15 to −20°C (most likely in the mixed-phase region), respectively. Even for the top 20% profiles, continental systems have convective cores with maximum radar reflectivity ~38 dBZ in the deep mixed-phase (−15°C). In contrast, monsoon (oceanic) convective systems have radar reflectivity near 30 (25) dBZ at the −15°C altitude. These differences on the vertical storm structures could explain the lightning activity distinction, as 35–40 dBZ around −15°C is a very good predictor of lighting discharge [*Williams et al.*, 2002; *Liu et al.*, 2012]. Only very extreme oceanic convection could loft hydrometeors large enough to have 35–40 dBZ

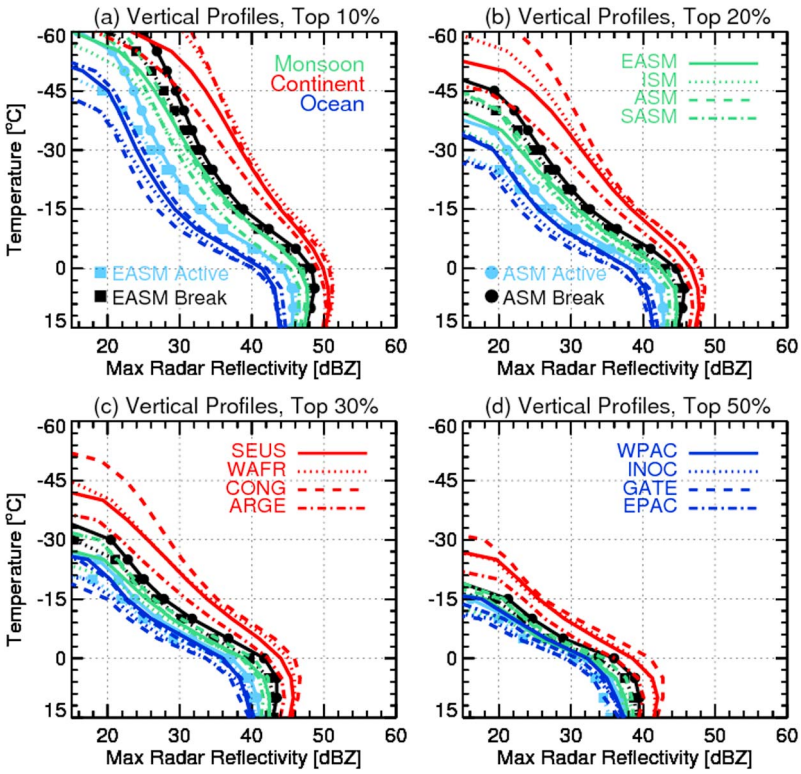

Figure 3. Vertical profiles of maximum radar reflectivity (at each altitude of a PF) as a function of NCEP temperature for precipitation systems in percentile of (a) top 10%, (b) top 20%, (c) top 30%, and (d) top 50%. Red, green, and blue curves represent continental, monsoon, oceanic regimes, respectively, while a set of active/break periods are shown by curves with filled squares or circles.

radar echoes around −15°C thus far less oceanic lightning [*Zipser*, 1994]. Over the tropical ocean, though the convection can extend to very high altitude ("hot towers") the convection intensity or updraft in the middle level is much weaker than that of continental or monsoon convection [*Zipser*, 2003; *Kelley et al.*, 2010]. Though the median radar vertical profiles come together, it does not mean the convective structures are similar on average for all rainfall regimes. The precipitation feature database is actually dominated (>80%) by small features (e.g., <400 km^2) that may be mostly weak in convection intensity [*Liu et al.*, 2008].

[13] Ice scattering signature from microwave measurements (37-GHz) indicates regime differences on populations of large ice particles aloft, e.g., hail or large graupel (Figure 4). Continental deep convection (top 10% PFs by 20-dBZ maximum height) exhibits much colder 37-GHz PCT indicating higher fraction of graupel or hail. Recent work by *Cecil* [2011] and *Cecil and Blankenship* [2012] has confirmed long-held suspicions by many that the 8 mm wavelength of 37-GHz is a superior indicator of scattering by large ice particles than 3 mm (85-GHz). According to these studies, low values of 37-GHz PCT coincide with hail occurrence. For example, 50, 30, 10 percent events have hail reports at the ground when 37-GHz PCT is below 180, 220, 260 K, respectively. If the moderate threshold (e.g., 220 K) of hail indicator is applied to this study, 35–40% of continental deep convective systems may produce hail at the ground, and most likely an even larger fraction in the mixed-phase region. In contrast, 10–20% of monsoon deep convection generates hail/graupel, while hail production is extremely rare in maritime systems even lower threshold (e.g., 240 K) is applied.

3.3. Convection Types and Structures of Monsoon Actives and Breaks

[14] Convection of monsoon actives is indeed different in properties from that during breaks in the same sense as has been documented in the literature on rainfall contribution by vigorous mixed-phase processes or lightning (Figures 2c and 2d), as well as convective vertical structures (Figures 3a and 3b). That is, convection during monsoon active periods is

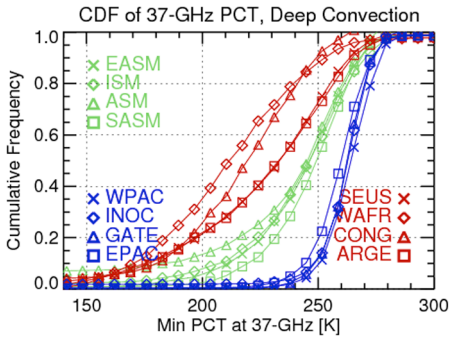

Figure 4. Cumulative distribution frequency (CDF) of deep convection (defined as top 10% PFs by maximum height of 20-dBZ) populations categorized by minimum 37-GHz PCT in continental (red curves), monsoon (green curves), oceanic (blue curves) regimes.

closer to that in oceanic regimes, and convection during breaks is a little closer to that in continental regimes. For example, during the active phases of the Australian monsoon, only 10% of rainfall comes from intense convection (e.g., 40 dBZ at 7 km), and 40% from systems with lightning. However, during break periods, the Australian monsoon has 30% of rainfall contributed by intense convection and 50% by thunderstorms. For the top 10% of radar vertical profiles, monsoon breaks have reflectivity close to 40 dBZ at −15°C, while monsoon active periods have less than 35 dBZ (a threshold for charge separation) radar echoes at the same temperature. Previous studies show that convective vertical structure, convective rainfall rates, and lightning activity are all more pronounced during break (easterly) periods than active (westerly) periods on regional scale [*Petersen et al.*, 2002; *Rickenbach et al.*, 2002; *May and Ballinger*, 2007; *Xu et al.*, 2009; *Lang et al.*, 2010] or case-by-case [*Cifelli et al.*, 2002; *Williams et al.*, 2002]. Changes in thermodynamics (i.e., CAPE and CIN) and aerosol concentration (i.e., CCN) are thought to be responsible for the observed regime-dependent convective structures of monsoon convection [*Williams et al.*, 2002].

4. Discussion and Conclusions

[15] This study quantifies convection types and structures in three classic tropical rainfall regimes, as well as the active and break periods of two monsoon regimes. Findings of regime variations are quite consistent with previous studies but here are extended to a 13-year database. Convection of continental rainfall is more intense (e.g., higher radar reflectivity through a deep layer and greater lightning flashrates) and mainly involves robust mixed-phase microphysical processes, less for monsoon convection, and least for oceanic convection. Major regime variations on convective structures are related to the mixed-phase dynamics (updraft) and microphysics, rather than the cloud depth or ice depth. Major microphysical processes involved in the continental regime are hail or graupel production in the mixed-phase region melting into large raindrops after descending below the freezing level. Maritime rainfall likely has a more significant contribution from low-level warm-rain collision and coalescence processes, though ice-based processes are still important. Land/ocean regime variations are related to thermodynamics (difference on CAPE and CIN) [*Rosenfeld and Lensky*, 1998; *Williams and Stanfill*, 2002], or aerosol effects (changes on CCN may modify cloud/precipitation microphysics) [*Rosenfeld and Lensky*, 1998; *Williams et al.*, 2002], or morphology of convective core (e.g., dilution of vertical motion is related to size of updraft) [*Zipser*, 2003; *Kelley et al.*, 2010]. The separation of monsoon regime from continental and oceanic rainfall regimes is also quite evident, though individual cases of convective structures and microphysics in the monsoon could be either continental-like or oceanic-like. Not all the monsoon systems are similar. North American Summer Monsoon (not shown) convection mostly resembles continental, while the Amazonian convection during the wet season shows properties that are closer to oceanic convection. Some regions such as West Africa contain a mixture of convective systems with different morphologies. For example, the northern portion of the West African region is dominated by squall lines with very intense convection, while the southern portion exhibits a more embedded convective MCS typology during JJA [*Zipser*, 1994; *Fink et al.*, 2006; *Guy and Rutledge*, 2012].

[16] Major conclusions from this study include: (1) Continental, monsoonal, and oceanic rainfall are clearly separated in the nature of their convection: intense convection or strong mixed-phase microphysical processes producing lightning contributes 80% (40%) of rainfall for continental (monsoon) regime, and less than 10% for oceanic regime. (2) Convective vertical structures and signatures of scattering by large ice particles show dramatic regime separation among continental and oceanic regimes with continental regime at the strongest end, oceanic at the weakest end, and monsoon regimes in the middle. (3) Regime variations on convective properties and structures within the monsoon context are also quite significant: their active periods are closer to oceanic regimes and their break periods are a little closer to continental regimes.

[17] **Acknowledgments.** This research was supported by the NASA Precipitation Measurement Mission grant NNX10AG90G, Program Manager Ramesh Kakar. Special thanks go to Chuntao Liu for creating and continually improving the TRMM precipitation features database.

[18] The Editor thanks the two anonymous reviewers for their assistance in evaluating this paper.

References

Arakawa, A. (2004), The cumulus parameterization problem: Past, present, and future, *J. Clim.*, *17*, 2493–2525, doi:10.1175/1520-0442(2004)017<2493:RATCPP>2.0.CO;2.

Cecil, D. J. (2011), Relating passive 37-GHz scattering to radar profiles in strong convection, *J. Appl. Meteorol. Climatol.*, *50*, 233–240, doi:10.1175/2010JAMC2506.1.

Cecil, D. J., and C. B. Blankenship (2012), Toward a global climatology of severe hailstorms as estimated by satellite passive microwave imagers, *J. Clim.*, *25*, 687–703, doi:10.1175/JCLI-D-11-00130.1.

Chang, C.-P. (2004), *East Asian Monsoon*, 564 pp., World Sci., Singapore.

Cifelli, R., W. A. Petersen, L. D. Carey, S. A. Rutledge, and M. A. F. da Silva Dias (2002), Radar observations of the kinematic, microphysical, and precipitation characteristics of two MCSs in TRMM LBA, *J. Geophys. Res.*, *107*(D20), 8077, doi:10.1029/2000JD000264.

Fink, A. H., D. G. Vincent, and V. Ermert (2006), Rainfall types in the West African Sudanian zone during the summer monsoon 2002, *Mon. Weather Rev.*, *134*(8), 2143–2164, doi:10.1175/MWR3182.1.

Gadgil, S. (2003), The Indian monsoon and its variability, *Annu. Rev. Earth Planet. Sci.*, *31*, 429–467, doi:10.1146/annurev.earth.31.100901.141251.

Guy, N., and S. A. Rutledge (2012), Regional comparison of West African convective characteristics: A TRMM-based climatology, *Q. J. R. Meteorol. Soc.*, doi:10.1002/qj.1865, in press.

Kelley, O. A., J. Stout, M. Summers, and E. J. Zipser (2010), Do the tallest convective cells over the tropical ocean have slow updrafts?, *Mon. Weather Rev.*, *138*, 1651–1672, doi:10.1175/2009MWR3030.1.

Lang, S., W.-K. Tao, J. Simpson, R. Cifelli, S. Rutledge, W. Olson, and J. Halverson (2007), Improving simulations of convective systems from TRMM LBA: Easterly and westerly regimes, *J. Atmos. Sci.*, *64*, 1141–1164, doi:10.1175/JAS3879.1.

Lang, T. J., S. A. Rutledge, and R. Cifelli (2010), Polarimetric radar observations of convection in northwestern Mexico during the North American Monsoon Experiment, *J. Hydrometeorol.*, *11*(6), 1345–1357, doi:10.1175/2010JHM1247.1.

Liu, C., E. J. Zipser, D. J. Cecil, S. W. Nesbitt, and S. Sherwood (2008), A cloud and precipitation feature database from nine years of TRMM observations, *J. Appl. Meteorol.*, *47*, 2712–2728, doi:10.1175/2008JAMC1890.1.

Liu, C., D. J. Cecil, E. J. Zipser, K. Kronfeld, and R. E. Robertson (2012), Relationships between lightning flash rates and radar reflectivity vertical structures in thunderstorms over the tropics and subtropics, *J. Geophys. Res.*, doi:10.1029/2011JD017123, in press.

Mapes, B. E., and R. A. Houze Jr. (1995), Diabatic divergence profiles in western Pacific mesoscale convective systems, *J. Atmos. Sci.*, *52*, 1807–1828, doi:10.1175/1520-0469(1995)052<1807:DDPIWP>2.0.CO;2.

May, P. T., and A. Ballinger (2007), The statistical characteristics of convective cells in a monsoon regime (Darwin, northern Australia), *Mon. Weather Rev.*, *135*(1), 82–92, doi:10.1175/MWR3273.1.

Mohr, K. I., and E. J. Zipser (1996), Mesoscale convective systems defined by their 85-GHz ice scattering signature: Size and intensity comparison over tropical oceans and continents, *Mon. Weather Rev.*,

124, 2417–2437, doi:10.1175/1520-0493(1996)124<2417:MCSDBT>2.0.CO;2.

Petersen, W. A., and S. A. Rutledge (2001), Regional variability in tropical convection: Observations from TRMM, *J. Clim.*, *14*, 3566–3586, doi:10.1175/1520-0442(2001)014<3566:RVITCO>2.0.CO;2.

Petersen, W. A., S. W. Nesbitt, R. J. Blakeslee, R. Cifelli, P. Hein, and S. A. Rutledge (2002), TRMM observations of intraseasonal variability in convective regimes over the Amazon, *J. Clim.*, *15*, 1278–1294, doi:10.1175/1520-0442(2002)015<1278:TOOIVI>2.0.CO;2.

Rickenbach, T. M., R. N. Ferreira, J. B. Halverson, D. L. Herdies, and M. A. F. Silva Dias (2002), Modulation of convection in the southwestern Amazon basin by extratropical stationary fronts, *J. Geophys. Res.*, *107*(D20), 8040, doi:10.1029/2000JD000263.

Riehl, H., and J. S. Simpson (1979), The heat balance in the equatorial trough zone, revisited, *Contrib. Atmos. Phys.*, *52*, 287–305.

Rosenfeld, D., and I. M. Lensky (1998), Satellite-based insights into precipitation formation processes in continental and maritime convective clouds, *Bull. Am. Meteorol. Soc.*, *79*, 2457–2476, doi:10.1175/1520-0477(1998)079<2457:SBIIPF>2.0.CO;2.

Suppiah, R. (1992), The Australian monsoon: A review, *Prog. Phys. Geogr.*, *16*, 283–318, doi:10.1177/030913339201600302.

Tao, W.-K., J. Simpson, S. Lang, M. McCumber, R. Adler, and R. Penc (1990), An algorithm to estimate the heating budget from vertical hydrometeor profiles, *J. Appl. Meteorol.*, *29*, 1232–1244, doi:10.1175/1520-0450(1990)029<1232:AATETH>2.0.CO;2.

Varble, A., et al. (2011), Evaluation of cloud-resolving model intercomparison simulations using TWP-ICE observations: Precipitation and cloud structure, *J. Geophys. Res.*, *116*, D12206, doi:10.1029/2010JD015180.

Williams, E. R., et al. (2002), Contrasting convective regimes over the Amazon: Implications for cloud electrification, *J. Geophys. Res.*, *107*(D20), 8082, doi:10.1029/2001JD000380.

Williams, E. R., and S. Stanfill (2002), The physical origin of the land–ocean contrast in lightning activity, *C. R. Phys.*, *3*, 1277–1292, doi:10.1016/S1631-0705(02)01407-X.

Xu, W., E. J. Zipser, and C. Liu (2009), Rainfall characteristics and convective properties of Mei-Yu precipitation systems over south China, Taiwan and the South China Sea. Part I: TRMM observations, *Mon. Weather Rev.*, *137*, 4261–4275, doi:10.1175/2009MWR2982.1.

Zhou, J., and K.-M. Lau (1998), Does a monsoon climate exist over South America?, *J. Clim.*, *11*, 1020–1040, doi:10.1175/1520-0442(1998)011<1020:DAMCEO>2.0.CO;2.

Zipser, E. J. (1994), Deep cumulonimbus cloud systems in the tropics with and without lightning, *Mon. Weather Rev.*, *122*, 1837–1851, doi:10.1175/1520-0493(1994)122<1837:DCCSIT>2.0.CO;2.

Zipser, E. J. (2003), Some views on "hot towers" after 50 years of tropical field programs and two years of TRMM data, *Meteorol. Monogr.*, *29*, 49, doi:10.1175/0065-9401(2003)029<0049:CSVOHT>2.0.CO;2.

Zipser, E. J., and K. R. Lutz (1994), The vertical profile of radar reflectivity of convective cells: A strong indicator of storm intensity and lightning probability?, *Mon. Weather Rev.*, *122*, 1751–1759, doi:10.1175/1520-0493(1994)122<1751:TVPORR>2.0.CO;2.

Zipser, E. J., D. J. Cecil, C. Liu, S. W. Nesbitt, and D. P. Yorty (2006), Where are the most intense thunderstorms on Earth?, *Bull. Am. Meteorol. Soc.*, *87*, 1057–1071, doi:10.1175/BAMS-87-8-1057.

W. Xu, Earth System Science Interdisciplinary Center, University of Maryland, 5825 University Research Ct., College Park, MD 20740-3823, USA. (wxinxu@umd.edu)

E. J. Zipser, Department of Atmospheric Sciences, University of Utah, 135 S. 1460 East, Room 819, Salt Lake City, UT 84112, USA.